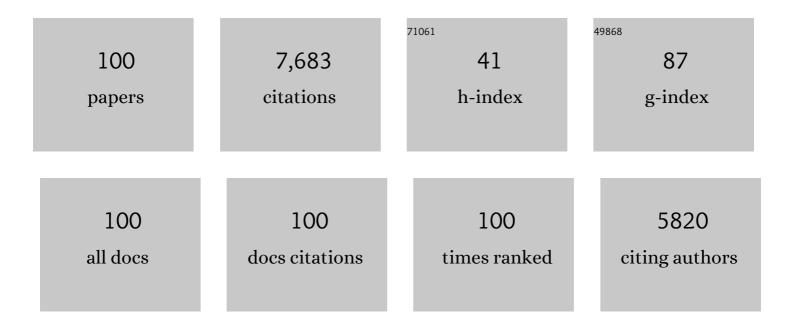
List of Publications by Year in descending order

Source: https://exaly.com/author-pdf/838964/publications.pdf Version: 2024-02-01



#	Article	IF	CITATIONS
1	Prostate Cancer: Multiparametric MR Imaging for Detection, Localization, and Staging. Radiology, 2011, 261, 46-66.	3.6	618
2	Relationship between Apparent Diffusion Coefficients at 3.0-T MR Imaging and Gleason Grade in Peripheral Zone Prostate Cancer. Radiology, 2011, 259, 453-461.	3.6	537
3	Prostate Cancer Localization with Dynamic Contrast-enhanced MR Imaging and Proton MR Spectroscopic Imaging. Radiology, 2006, 241, 449-458.	3.6	506
4	Evaluation of prostate segmentation algorithms for MRI: The PROMISE12 challenge. Medical Image Analysis, 2014, 18, 359-373.	7.0	469
5	Discrimination of Prostate Cancer from Normal Peripheral Zone and Central Gland Tissue by Using Dynamic Contrast-enhanced MR Imaging. Radiology, 2003, 229, 248-254.	3.6	375
6	Magnetic Resonance Imaging Guided Prostate Biopsy in Men With Repeat Negative Biopsies and Increased Prostate Specific Antigen. Journal of Urology, 2010, 183, 520-528.	0.2	344
7	Computer-Aided Detection of Prostate Cancer in MRI. IEEE Transactions on Medical Imaging, 2014, 33, 1083-1092.	5.4	338
8	Prostate Cancer: Body-Array versus Endorectal Coil MR Imaging at 3 T—Comparison of Image Quality, Localization, and Staging Performance. Radiology, 2007, 244, 184-195.	3.6	295
9	Prospective Assessment of Prostate Cancer Aggressiveness Using 3-T Diffusion-Weighted Magnetic Resonance Imaging–Guided Biopsies Versus a Systematic 10-Core Transrectal Ultrasound Prostate Biopsy Cohort. European Urology, 2012, 61, 177-184.	0.9	277
10	The Medical Segmentation Decathlon. Nature Communications, 2022, 13, .	5.8	252
11	Staging Prostate Cancer with Dynamic Contrast-enhanced Endorectal MR Imaging prior to Radical Prostatectomy: Experienced versus Less Experienced Readers. Radiology, 2005, 237, 541-549.	3.6	223
12	Volumetric breast density estimation from full-field digital mammograms. IEEE Transactions on Medical Imaging, 2006, 25, 273-282.	5.4	208
13	IMRT boost dose planning on dominant intraprostatic lesions: Gold marker-based three-dimensional fusion of CT with dynamic contrast-enhanced and 1H-spectroscopic MRI. International Journal of Radiation Oncology Biology Physics, 2006, 65, 291-303.	0.4	168
14	Assessment of Prostate Cancer Aggressiveness Using Dynamic Contrast-enhanced Magnetic Resonance Imaging at 3 T. European Urology, 2013, 64, 448-455.	0.9	152
15	Initial Experience of 3 Tesla Endorectal Coil Magnetic Resonance Imaging and 1H-Spectroscopic Imaging of the Prostate. Investigative Radiology, 2004, 39, 671-680.	3.5	148
16	Imaging vascular function for early stage clinical trials using dynamic contrast-enhanced magnetic resonance imaging. European Radiology, 2012, 22, 1451-1464.	2.3	138
17	Automated Assessment of COVID-19 Reporting and Data System and Chest CT Severity Scores in Patients Suspected of Having COVID-19 Using Artificial Intelligence. Radiology, 2021, 298, E18-E28.	3.6	116
18	Accurate estimation of pharmacokinetic contrast-enhanced dynamic MRI parameters of the prostate. Journal of Magnetic Resonance Imaging, 2001, 13, 607-614.	1.9	106

#	Article	IF	CITATIONS
19	Thirty-Two-Channel Coil 3T Magnetic Resonance-Guided Biopsies of Prostate Tumor Suspicious Regions Identified on Multimodality 3T Magnetic Resonance Imaging: Technique and Feasibility. Investigative Radiology, 2008, 43, 686-694.	3.5	104
20	Prostate Cancer: Computer-aided Diagnosis with Multiparametric 3-T MR Imaging—Effect on Observer Performance. Radiology, 2013, 266, 521-530.	3.6	103
21	PROSTATEx Challenges for computerized classification of prostate lesions from multiparametric magnetic resonance images. Journal of Medical Imaging, 2018, 5, 1.	0.8	98
22	The effect of an endorectal balloon and off-line correction on the interfraction systematic and random prostate position variations: A comparative study. International Journal of Radiation Oncology Biology Physics, 2005, 61, 278-288.	0.4	95
23	Computer-assisted analysis of peripheral zone prostate lesions using T2-weighted and dynamic contrast enhanced T1-weighted MRI. Physics in Medicine and Biology, 2010, 55, 1719-1734.	1.6	93
24	Computerized analysis of prostate lesions in the peripheral zone using dynamic contrast enhanced MRI. Medical Physics, 2008, 35, 888-899.	1.6	81
25	End-to-end prostate cancer detection in bpMRI via 3D CNNs: Effects of attention mechanisms, clinical priori and decoupled false positive reduction. Medical Image Analysis, 2021, 73, 102155.	7.0	74
26	Standardized Threshold Approach Using Three-Dimensional Proton Magnetic Resonance Spectroscopic Imaging in Prostate Cancer Localization of the Entire Prostate. Investigative Radiology, 2007, 42, 116-122.	3.5	70
27	Interpatient Variation in Normal Peripheral Zone Apparent Diffusion Coefficient: Effect on the Prediction of Prostate Cancer Aggressiveness. Radiology, 2012, 265, 260-266.	3.6	66
28	Computer-Aided Lesion Diagnosis in Automated 3-D Breast Ultrasound Using Coronal Spiculation. IEEE Transactions on Medical Imaging, 2012, 31, 1034-1042.	5.4	63
29	Evaluation of a robotic technique for transrectal MRI-guided prostate biopsies. European Radiology, 2012, 22, 476-483.	2.3	60
30	Prostate Cancer: Precision of Integrating Functional MR Imaging with Radiation Therapy Treatment by Using Fiducial Gold Markers. Radiology, 2005, 236, 311-317.	3.6	58
31	Clinical evaluation of a computer-aided diagnosis system for determining cancer aggressiveness in prostate MRI. European Radiology, 2015, 25, 3187-3199.	2.3	57
32	Feasibility of 3T Dynamic Contrast-Enhanced Magnetic Resonance-Guided Biopsy in Localizing Local Recurrence of Prostate Cancer After External Beam Radiation Therapy. Investigative Radiology, 2010, 45, 121-125.	3.5	56
33	Precision and accuracy of acoustospectrographic parameters. Ultrasound in Medicine and Biology, 1996, 22, 855-871.	0.7	55
34	Contrast-enhanced magnetic resonance imaging of the breast: the value of pharmacokinetic parameters derived from fast dynamic imaging during initial enhancement in classifying lesions. European Radiology, 2008, 18, 1123-1133.	2.3	54
35	A Pattern Recognition Approach to Zonal Segmentation of the Prostate on MRI. Lecture Notes in Computer Science, 2012, 15, 413-420.	1.0	50
36	Elastic Versus Rigid Image Registration in Magnetic Resonance Imaging–transrectal Ultrasound Fusion Prostate Biopsy: A Systematic Review and Meta-analysis. European Urology Focus, 2018, 4, 219-227.	1.6	49

#	Article	lF	CITATIONS
37	A Novel Deep Learning Based Computer-Aided Diagnosis System Improves the Accuracy and Efficiency of Radiologists in Reading Biparametric Magnetic Resonance Images of the Prostate. Investigative Radiology, 2021, 56, 605-613.	3.5	49
38	Deep learning–assisted prostate cancer detection on bi-parametric MRI: minimum training data size requirements and effect of prior knowledge. European Radiology, 2022, 32, 2224-2234.	2.3	48
39	Computer-extracted Features Can Distinguish Noncancerous Confounding Disease from Prostatic Adenocarcinoma at Multiparametric MR Imaging. Radiology, 2016, 278, 135-145.	3.6	43
40	Artificial Intelligence Based Algorithms for Prostate Cancer Classification and Detection on Magnetic Resonance Imaging: A Narrative Review. Diagnostics, 2021, 11, 959.	1.3	43
41	Simulated required accuracy of image registration tools for targeting high-grade cancer components with prostate biopsies. European Radiology, 2013, 23, 1401-1407.	2.3	41
42	Multiparametric MRI and auto-fixed volume of interest-based radiomics signature for clinically significant peripheral zone prostate cancer. European Radiology, 2020, 30, 1313-1324.	2.3	40
43	Evaluation of Image Registration in PET/CT of the Liver and Recommendations for Optimized Imaging. Journal of Nuclear Medicine, 2007, 48, 910-919.	2.8	39
44	Correlation between dynamic contrast-enhanced MRI and quantitative histopathologic microvascular parameters in organ-confined prostate cancer. European Radiology, 2014, 24, 2597-2605.	2.3	38
45	Inter-site Variability in Prostate Segmentation Accuracy Using Deep Learning. Lecture Notes in Computer Science, 2018, , 506-514.	1.0	37
46	Segmentation of the Heart Muscle in 3-D Pediatric Echocardiographic Images. Ultrasound in Medicine and Biology, 2007, 33, 1453-1462.	0.7	36
47	MRI to X-ray mammography intensity-based registration with simultaneous optimisation of pose and biomechanical transformation parameters. Medical Image Analysis, 2014, 18, 674-683.	7.0	36
48	Supervised Uncertainty Quantification for Segmentation with Multiple Annotations. Lecture Notes in Computer Science, 2019, , 137-145.	1.0	36
49	Retrospective comparison of direct in-bore magnetic resonance imaging (MRI)-guided biopsy and fusion-guided biopsy in patients with MRI lesions which are likely or highly likely to be clinically significant prostate cancer. World Journal of Urology, 2017, 35, 1849-1855.	1.2	35
50	ESUR/ESUI position paper: developing artificial intelligence for precision diagnosis of prostate cancer using magnetic resonance imaging. European Radiology, 2021, 31, 9567-9578.	2.3	34
51	1.5-T multiparametric MRI using PI-RADS: a region by region analysis to localize the index-tumor of prostate cancer in patients undergoing prostatectomy. Acta Radiologica, 2015, 56, 500-511.	0.5	33
52	Fully Automatic Deep Learning Framework for Pancreatic Ductal Adenocarcinoma Detection on Computed Tomography. Cancers, 2022, 14, 376.	1.7	30
53	Automated analysis of contrast enhancement in breast MRI lesions using mean shift clustering for ROI selection. Journal of Magnetic Resonance Imaging, 2007, 26, 606-614.	1.9	29
54	Clinical validation of the normalized mutual information method for registration of CT and MR images in radiotherapy of brain tumors. Journal of Applied Clinical Medical Physics, 2004, 5, 66-79.	0.8	27

#	Article	IF	CITATIONS
55	MRI to X-ray mammography registration using a volume-preserving affine transformation. Medical Image Analysis, 2012, 16, 966-975.	7.0	26
56	Computerized whole slide quantification shows increased microvascular density in pT2 prostate cancer as compared to normal prostate tissue. Prostate, 2009, 69, 62-69.	1.2	25
57	Multi-Modal Siamese Network for Diagnostically Similar Lesion Retrieval in Prostate MRI. IEEE Transactions on Medical Imaging, 2021, 40, 986-995.	5.4	22
58	Initial Results of 3-Dimensional 1H-Magnetic Resonance Spectroscopic Imaging in the Localization of Prostate Cancer at 3 Tesla. Investigative Radiology, 2011, 46, 301-306.	3.5	21
59	Quantitative ultrasonic analysis of liver metastases. Ultrasound in Medicine and Biology, 1998, 24, 67-77.	0.7	20
60	Detection and PI-RADS classification of focal lesions in prostate MRI: Performance comparison between a deep learning-based algorithm (DLA) and radiologists with various levels of experience. European Journal of Radiology, 2021, 142, 109894.	1.2	20
61	Fast Scan Conversion Algorithms for Displaying Ultrasound Sector Images. Ultrasonic Imaging, 1994, 16, 87-108.	1.4	19
62	Comparison of enhancement characteristics between invasive lobular carcinoma and invasive ductal carcinoma. Journal of Magnetic Resonance Imaging, 2011, 34, 293-300.	1.9	19
63	Visibility of prostate cancer on transrectal ultrasound during fusion with multiparametric magnetic resonance imaging for biopsy. Clinical Imaging, 2016, 40, 745-750.	0.8	19
64	False Positive Reduction Using Multiscale Contextual Features for Prostate Cancer Detection in Multi-Parametric MRI Scans. , 2020, , .		19
65	Adaptive Texture Feature Extraction with Application to Ultrasonic Image Analysis. Ultrasonic Imaging, 1998, 20, 132-148.	1.4	18
66	Biomechanical modeling constrained surfaceâ€based image registration for prostate MR guided TRUS biopsy. Medical Physics, 2015, 42, 2470-2481.	1.6	18
67	Automated 3â€dimensional segmentation of pelvic lymph nodes in magnetic resonance images. Medical Physics, 2011, 38, 6178-6187.	1.6	17
68	Correlation Based 3-D Segmentation of the Left Ventricle in Pediatric Echocardiographic Images Using Radio-Frequency Data. Ultrasound in Medicine and Biology, 2011, 37, 1409-1420.	0.7	17
69	Single-center versus multi-center biparametric MRI radiomics approach for clinically significant peripheral zone prostate cancer. Insights Into Imaging, 2021, 12, 150.	1.6	15
70	Chest wall segmentation in automated 3D breast ultrasound scans. Medical Image Analysis, 2013, 17, 1273-1281.	7.0	12
71	Designing image segmentation studies: Statistical power, sample size and reference standard quality. Medical Image Analysis, 2017, 42, 44-59.	7.0	12
72	Lymph node detection in MR Lymphography: false positive reduction using multi-view convolutional neural networks. PeerJ, 2019, 7, e8052.	0.9	12

5

#	Article	lF	CITATIONS
73	Quantitative identification of magnetic resonance imaging features of prostate cancer response following laser ablation and radical prostatectomy. Journal of Medical Imaging, 2014, 1, 035001.	0.8	11
74	Prediction of prostate cancer grade using fractal analysis of perfusion MRI: retrospective proof-of-principle study. European Radiology, 2021, , 1.	2.3	11
75	A deep learning masked segmentation alternative to manual segmentation in biparametric MRI prostate cancer radiomics. European Radiology, 2022, 32, 6526-6535.	2.3	11
76	Automated Calibration for Computerized Analysis of Prostate Lesions Using Pharmacokinetic Magnetic Resonance Images. Lecture Notes in Computer Science, 2009, 12, 836-843.	1.0	9
77	Intranodal signal suppression in pelvic MR lymphography of prostate cancer patients: a quantitative comparison of ferumoxtran-10 and ferumoxytol. PeerJ, 2016, 4, e2471.	0.9	8
78	Correction of an image size difference between positron emission tomography (PET) and computed tomography (CT) improves image fusion of dedicated PET and CT. Nuclear Medicine Communications, 2006, 27, 515-519.	0.5	7
79	Combining T2-weighted with dynamic MR images for computerized classification of prostate lesions. , 2008, , .		7
80	3D Cardiac Segmentation Using Temporal Correlation of Radio Frequency Ultrasound Data. Lecture Notes in Computer Science, 2009, 12, 927-934.	1.0	7
81	MR-targeted TRUS prostate biopsy using local reference augmentation: initial experience. International Urology and Nephrology, 2016, 48, 1037-1045.	0.6	6
82	The Key Role of Patient Involvement in the Development of Core Outcome Sets in Prostate Cancer. European Urology Focus, 2021, 7, 943-946.	1.6	6
83	Sliced alternating DICOM series: convenient visualisation of image fusion on PACS. European Journal of Nuclear Medicine and Molecular Imaging, 2005, 32, 247-248.	3.3	5
84	Classification of breast lesions in automated 3D breast ultrasound. Proceedings of SPIE, 2011, , .	0.8	5
85	Computer aided analysis of breast MRI enhancement kinetics using mean shift c lustering and multifeature iterative region of interest selection. Journal of Magnetic Resonance Imaging, 2012, 36, 1104-1112.	1.9	5
86	Intensity-Based MRI to X-ray Mammography Registration with an Integrated Fast Biomechanical Transformation. Lecture Notes in Computer Science, 2012, , 48-55.	1.0	5
87	FEW-SHOT Image Segmentation for Cross-Institution Male Pelvic Organs Using Registration-Assisted Prototypical Learning. , 2022, , .		4
88	Breast MRI intensity non-uniformity correction using mean-shift. Proceedings of SPIE, 2010, , .	0.8	3
89	Accuracy of fractal analysis and PI-RADS assessment of prostate magnetic resonance imaging for prediction of cancer grade groups: a clinical validation study. European Radiology, 2022, 32, 2372-2383.	2.3	3

90 Surface-based prostate registration with biomechanical regularization. , 2013, , .

#	Article	IF	CITATIONS
91	Automated multistructure atlasâ€assisted detection of lymph nodes using pelvic MR lymphography in prostate cancer patients. Medical Physics, 2016, 43, 3132-3142.	1.6	2
92	Chestwall Segmentation in 3D Breast Ultrasound Using a Deformable Volume Model. , 2007, 20, 245-256.		2
93	Required Accuracy of MR-US Registration for Prostate Biopsies. Lecture Notes in Computer Science, 2011, , 92-99.	1.0	2
94	Computer Aided Detection of Prostate Cancer Using T2, DWI and DCE MRI: Methods and Clinical Applications. Lecture Notes in Computer Science, 2010, , 4-14.	1.0	1
95	<title>Accurate estimation of contrast agent dynamics in fast contrast-enhanced MRI</title> . , 2000, , .		Ο
96	Integrating biological knowledge, novel imaging modalities, and modeling in breast cancer diagnosis. , 2009, , .		0
97	Automated classification of lymph nodes in USPIO-enhanced MR-images: a comparison of three segmentation methods. , 2010, , .		Ο
98	Automated segmentation of reference tissue for prostate cancer localization in dynamic contrast enhanced MRI. Proceedings of SPIE, 2010, , .	0.8	0
99	Solid Science of Al Supporting Bladder Cancer CT Reading. Academic Radiology, 2019, 26, 1146-1147.	1.3	Ο
100	Statistical Power in Image Segmentation: Relating Sample Size to Reference Standard Quality. Lecture Notes in Computer Science, 2015, , 105-113.	1.0	0